Singlet extended standard model in the context of split supersymmetry

Martin Gabelmann[*] and M. Margarete Mühlleitner[†]

Institute for Theoretical Physics (ITP), Karlsruhe Institute of Technology,
Wolfgang-Gaede-Straße 1, D-76131 Karlsruhe, Germany

Florian Staub[‡]

Institute for Theoretical Physics (ITP), Karlsruhe Institute of Technology,
Wolfgang-Gaede-Straße 1, D-76131 Karlsruhe, Germany
and Institute for Nuclear Physics (IKP), Karlsruhe Institute of Technology,
Hermann-von-Helmholtz-Platz 1, D-76344 Eggenstein-Leopoldshafen, Germany

We consider a low-energy effective theory of the next-to-minimal supersymmetric Standard Model by decoupling all scalar states except one Higgs doublet and the complex gauge singlet. The mass spectrum of the resulting singlet extended Standard Model is calculated from two different perspectives: (i) using a matching of the scalar sectors at next-to-leading order and (ii) using the simplified-model approach of calculating the masses in the effective theory at fixed order at the weak scale ignoring any connection to the full theory. Significant deviations between the two methods are found not only in the scalar sector, but also properties of the additional fermions can be very different. Thus, only a small part of the parameter space of the simplified model can be embedded in a well-motivated supersymmetry framework.

I. INTRODUCTION

The discovery of the Higgs boson in 2012 with a mass of about $m_h \approx 125$ GeV [1–3] strengthens the question whether additional light spin-0 fields may exist in nature. Scalar fields transforming as singlets under the Standard Model (SM) gauge group appear in a variety of models beyond the SM (BSM). They can serve as mediators to hidden sectors or as dark matter (DM) candidates. In addition, their vacuum expectation value v (VEV) can help to understand the appearance of dimensionful parameters. However, models predicting singlet fields can originate from different theoretical motivations, formulated within different frameworks such as gauge-, gravity-, or anomaly-mediated supersymmetry (SUSY) breaking, extra dimensions, conformal field theory, compositeness, etc., as well as admixtures. Thus, the hypothetical discovery of a singlet scalar would not necessarily point to a specific class of models. On the other hand, there are increasing experimental constraints on e.g., color-charged BSM fields [4] that may appear along the weaker constrained singlet states.

Therefore, a common approach to study singlet extensions is to be as generic as possible: after integrating out all heavy degrees of freedom (d.o.f.), the resulting low-energy effective field theory (EFT) is considered without any connection to the fundamental theory. In this way, parameter scans of the "simplified model" can cover many different classes of theories. However, this ansatz not only neglects possible correlations among the parameters, but also might include parameter regions that are not accessible by any reasonable full theory. Moreover, it is not even clear if all other BSM particles predicted by the ultraviolet (UV) theory but the singlet can be decoupled in a consistent way. Therefore, it is interesting to ask which part of the parameter space of a simplified model is accessible when assuming a concrete UV completion. In order to address this question, a precise matching of the two theories as well as the evaluation of the renormalization group equations (RGEs) is required.

In this context, we are going to consider the singlet extended SM (SSM) as EFT of the next-to-minimal supersymmetric Standard Model (NMSSM). This constellation is a new variant of the popular ideas of high-scale or split SUSY [5] which usually consider the minimal supersymmetric Standard Model (MSSM) with a specific R-symmetry-breaking pattern [6,7] as full theory in the UV. Split SUSY has the advantage of providing a dark

[*]martin.gabelmann@kit.edu
[†]milada.muehlleitner@kit.edu
[‡]florian.staub@kit.edu

matter candidate and improving the unification of the SM gauge couplings compared to low-scale SUSY scenarios [8]. In addition, nonminimal split SUSY can be connected to cosmological observables such as baryon asymmetry [9,10] or gravitational waves [11]. As we will discuss, the considered singlet extension of the MSSM does not allow one to decouple the electroweakinos while keeping the singlet light, which is why a purely scalar-singlet extension of the SM can only hardly be motivated by nonminimal SUSY.

In general, the presence of additional heavy states in the UV theory makes the inclusion of higher-order corrections to the matching conditions mandatory in order to keep the theoretical uncertainties under control [12–16]. The higher-order effects in the matching of the high-scale MSSM, where all BSM states are very heavy, to the SM can alter the Higgs mass by several GeV [16]. Moreover, one needs to include carefully the effects of potentially light states. This has been discussed for instance in the context of the two Higgs doublet model as a low-energy theory of the MSSM [17–23]: it was shown that the SM-like Higgs boson mass prediction using a proper decoupling of heavy—and only heavy—scalars can differ by up to 10 GeV compared to simple high-scale SUSY approaches which also treat the second Higgs doublet as if it would be heavy. On the other side, the impact of higher-dimensional operators is usually subdominant for the Higgs boson mass prediction. It was shown for the MSSM that the impact of dimension-six operators, scaling with $\mathcal{O}(v_{\mathrm{SM}}^2/M_{\mathrm{SUSY}}^2)$, on the Higgs boson mass becomes very weak if the BSM scale is above 1–2 TeV [14]. Thus contributions of higher-dimensional operators are negligible for this work, because we require not only the SM VEV to be smaller than the decoupling scale, $v_{\mathrm{SM}} \ll M_{\mathrm{SUSY}}$, but also the VEV of the additional (light) singlet v_s must be comparable to the singlet mass to get a consistent effective theory and a stable potential.

The remainder of the paper is organized as follows. In Sec. II, the NMSSM is introduced focusing on the soft SUSY-breaking scalar part as well as the resulting properties of the low-energy model, the SSM. Section III discusses higher-order effects that arise when couplings with positive mass dimension are involved in the matching. In Sec. IV, we compare the simplified model with the matching approach. Conclusions and outlooks are given in Sec. V.

II. HOW DOES A SSM EMERGE FROM SUSY?

Simplified models that involve additional scalars are often motivated by SUSY because a consistent and phenomenological viable SUSY model needs at least one additional doublet. Thus, simplified models assume that SUSY contributes with only very few new d.o.f. at the weak scale, but all other positive aspects of the full theory, like diminishing the hierarchy problem, come into play at a higher scale [24–29]. However, this means that all additional states predicted by SUSY need to decouple in a consistent way. As we will show, this is not always possible since assumptions such as the introduction of discrete symmetries in the scalar sector are not compatible with those predicted by SUSY and specific soft-SUSY-breaking patterns. In addition, the inclusion of higher-order corrections shows that it is not possible to enforce a large mass hierarchy between specific states without decoupling the singlet as well. We want to discuss this at the example of matching the NMSSM to the SSM.

A. Possible low-energy limits from the NMSSM

There is a rich collection of motivations and introductions for the softly broken (N)MSSM available in the literature; see for instance Refs. [30–32] and references therein. Therefore, we skip the motivation and continue with the discussion of how to obtain a low-energy limit of the NMSSM that involves (at least) one scalar gauge singlet. The most general[1] superpotential of the NMSSM without assuming any global symmetry is

$$\mathcal{W}_{\mathrm{NMSSM}} = \mathcal{W}_{\mathrm{MSSM}} + M_S \hat{S}^2 + \lambda \hat{S} \hat{H}_u \cdot \hat{H}_d + \frac{\kappa}{3} \hat{S}^3, \quad (1)$$

with

$$\begin{aligned}
\mathcal{W}_{\mathrm{MSSM}} = {} & \mu \hat{H}_u \cdot \hat{H}_d + Y_u \hat{H}_u \cdot \hat{Q}\, \hat{u} \\
& + Y_d \hat{H}_d \cdot \hat{Q}\, \hat{d} + Y_e \hat{H}_e \cdot \hat{L}\, \hat{e},
\end{aligned} \quad (2)$$

where we follow the notation of [33]. The corresponding soft-SUSY-breaking terms are

$$L_{\mathrm{NMSSM}}^{\mathrm{soft}} = L_{\mathrm{MSSM}}^{\mathrm{soft}} + tS + B_S S^2 + T_\lambda S H_u \cdot H_d + \frac{T_\kappa}{3} S^3,$$
$$(3)$$

with

$$L_{\mathrm{MSSM}}^{\mathrm{soft}} = B_\mu H_u \cdot H_d + T_u H_u \cdot \tilde{Q}\, \tilde{u} + T_d H_d \cdot \tilde{Q}\, \tilde{d} + T_e H_e \cdot \tilde{L}\, \tilde{e}$$
$$(4)$$

and the soft-breaking scalar mass squared terms $m_\phi^2 |\phi|^2$ for all scalars $\phi = \{H_d, H_u, S, \tilde{Q}, \tilde{u}, \tilde{d}, \tilde{L}, \tilde{e}\}$ as well as soft fermion masses $M_{\lambda=1,2,3}$ for the bino ($\tilde{B}$), wino ($\tilde{W}$) and the gluino ($\tilde{g}$).

The low-energy theory shall contain a complex singlet. The most general scalar potential involving a complex singlet is

---

[1]The absence of a tadpole term in Eq. (1) is due to a redefinition of the singlet field such that only a soft-breaking tadpole in Eq. (3) remains.
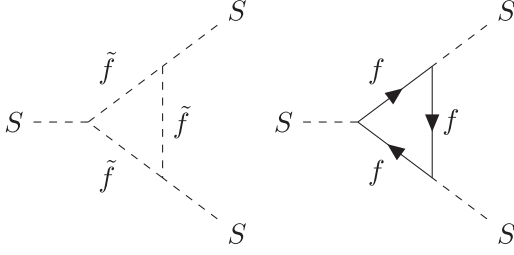
FIG. 1.   Generic one-loop contribution of a scalar (fermion) $\tilde{f}$ (f) to the trilinear scalar self-coupling. While the scalar contribution scales as [Trilinear coupling]$^3/m_{\tilde{f}}^2 \xrightarrow{m_{\tilde{f}} \to \infty} 0$, the fermionic contribution, [Yukawa coupling]$^3 \, m_f$, does not decouple in the limit $m_f \to \infty$.

$$V(H,S) = m_H^2 HH^\dagger + \frac{\lambda_H}{2}|HH^\dagger|^2 + m_S^2|S|^2 + (\tilde{m}_S^2 S^2 + \text{H.c.})$$
$$+ \frac{\lambda_S}{2}|S|^4 + (\lambda_S'|S|^2 S^2 + \lambda_S'' S^4 + \text{H.c.})$$
$$+ \lambda_{SH}|S|^2 HH^\dagger + (\lambda_{SH}' S^2 HH^\dagger + \text{H.c.})$$
$$+ (\kappa_{SH} SHH^\dagger + \kappa_S SSS + \kappa_S'|S|^2 S + \text{H.c.}). \quad (5)$$

For consistency reasons (such as vacuum stability) all dimensionful parameters in this potential as well as the two VEVs v and v_S of the doublet H and the singlet S must be roughly of the same size. It seems that Eqs. (1)–(4) provide enough freedom to decouple all squarks, sleptons, the second doublet, electroweakinos, and the singlino. However, this is only correct at leading order. At one-loop order, trilinear self-couplings would receive corrections from heavy fermions and scalars depicted in Fig. 1. For instance, the trilinear self-coupling κ_S will receive loop corrections at the matching scale involving the singlino ($f = \tilde{S}$ in the right diagram of Fig. 1) that scale with

$$\kappa_S^{\text{one loop}} \sim \kappa^3 m_{\tilde{S}}, \quad (6)$$

where κ and $m_{\tilde{S}}$ is the Yukawa coupling and mass of the singlino. Therefore, $\tilde{S}$ would not decouple from the low-energy Lagrangian in the limit $m_{\tilde{S}} \to \infty$. Similarly, the coupling κ_{SH} receives loop corrections from Higgsino or gaugino loops, e.g.,

$$\kappa_{SH}^{\text{one loop}} \sim g_i^2 \lambda (M_i + m_{\tilde{H}_{u,d}})$$
$$+ \kappa\lambda^2 (m_{\tilde{S}} + m_{\tilde{H}_{u,d}}), \quad i = \{1,2\}, \quad (7)$$

where λ is the singlet-Higgsino-Higgsino coupling and g_i the Higgs-Higgsino-gaugino coupling.

Thus, all additional SUSY fermions that couple to the singlet must have masses similar to the scalar singlet in order to ensure trilinear couplings of the order of the low-energy scale. On the other hand, scalar contributions to trilinear couplings, shown in the left diagram of Fig. 1,

always decouple. Therefore, the second doublet as well as the squarks and sleptons can be kept heavy by assuming the soft-squared parameters B_μ and $m_{\tilde{f}}^2$, $\tilde{f} = \{\tilde{Q}, \tilde{U}, \tilde{e}, \tilde{d}, \tilde{u}\}$ to be much larger than the electroweak scale.

Neglecting for the moment the effect of singlet-doublet mixing we can easily calculate the masses $m_{\phi_s}^2$, m_σ^2 of the CP-even and -odd component of the singlet. In the limit $t, v \to 0$ these are given by

$$m_{\phi_s}^2 = \frac{3}{\sqrt{2}}\kappa M_S v_S + \frac{1}{\sqrt{2}}v_S T_\kappa + 2\kappa^2 v_S^2, \quad (8)$$

$$m_\sigma^2 = -2B_S - \frac{1}{\sqrt{2}}v_S(\kappa M_S + 3T_\kappa). \quad (9)$$

Thus, taking $|B_S|$ to be very large, too, would also decouple the CP-odd component of the singlet and result in the SM extended by a real singlet as EFT. However, we are going to concentrate on the complex-singlet case. Based on these considerations, the hierarchy of dimensionful parameters used in the following can be summarized using two different scales:

$$\sqrt{B_S}, t, \mu, v_S, T_{\lambda,\kappa,\tilde{e},\tilde{d},\tilde{u}}, M_{S,1,2,3} \sim m_{\text{Sing}} \sim 1 \text{ TeV}, \quad (10)$$

$$B_\mu, m_{\tilde{l},\tilde{q},\tilde{u},\tilde{e},\tilde{d}}^2 \sim M_{\text{SUSY}}^2 \gg (1 \text{ TeV})^2. \quad (11)$$

In order to reduce the number of free parameters, we assume $t = M_S = \mu = B_S = 0$ for simplicity, which leads to a scale-invariant superpotential without a tadpole[2] problem [32]. There is—to our knowledge—no discrete (R) symmetry that would justify setting all mentioned parameters to zero simultaneously. However, these kind of parameters would anyways be neglected in the matching of our calculation, since they are suppressed by factors of M_{SUSY}^{-2}. Furthermore, μ is the only parameter that would lead to a new operator $\mu\tilde{H}_u\tilde{H}_d$ in the EFT in Eq. (20), which we do not consider because it mainly concerns the Higgsino masses but has minor effect on the singlino and scalar sector onto which we focus. For further simplification, we assume also the soft-sfermion mass matrices and trilinear couplings to be degenerate and flavor-diagonal:

$$T_{\tilde{i}} = Y_i A_0, \quad A_0 \approx \mathcal{O}(m_{\text{Sing}}), \quad i = u, d, e,$$
$$m_{\tilde{i}}^2 = \mathbb{1}M_{\text{SUSY}}^2, \quad i = \tilde{l}, \tilde{q}, \tilde{u}, \tilde{e}, \tilde{d}, \quad (12)$$

and only take the third-generation Yukawa couplings $Y_i^{(3,3)}$ into account. The additional Higgs boson states are automatically degenerate in the mass m_A in the decoupling limit:

---

[2] A nonzero tadpole t would also lead to a singlet mass that scales with t/v_S which would decouple the singlet for small values of v_S.

$$m_A^2 \xrightarrow{B_\mu \gg m_W^2} \frac{1 + \tan^2\beta}{\tan\beta} B_\mu. \tag{13}$$

With Eq. (11) it follows that $m_A^2 \sim \mathcal{O}(M_{\mathrm{SUSY}}^2)$; i.e., all heavy scalars have masses of the same size and can be decoupled at one matching scale in a consistent way. Thus, there are two additional BSM scales: M_{SUSY} in the UV and one intermediate mass scale $m_{\mathrm{Sing}} \ll M_{\mathrm{SUSY}}$ in the EFT. The latter can either be smaller or larger than v_{SM}. However, m_{Sing} should not be much larger than 1 TeV in order to keep it close to the SM scale and ensure the validity of the EFT approach.

B. The low-energy Lagrangian

As a result of Eqs. (10)–(13) only fermions, one Higgs doublet and one complex singlet do not decouple. Thus, the considered EFT consists of the SM complemented with a complex singlet scalar S as well as Weyl fermions transforming as SU(2) singlets $\tilde{S}$ (singlino), $\tilde{B}$ (bino), a pair of two $\mathrm{SU}(2) \times \mathrm{U}(1)$ doublets $\tilde{H}_u$ and $\tilde{H}_d$ (Higgsinos), a SU(2) triplet $\tilde{W}$ (wino) and an SU(3) octet $\tilde{g}$ (gluino).

To avoid confusion, we make use of the same notation for the fields in the EFT as we did in the NMSSM although they differ by a field renormalization. In order to simplify the following discussion, it turns out to be helpful to rewrite the complex singlet into a pair of real CP-even and -odd components:

$$S = \frac{1}{\sqrt{2}}(S_r + iS_i), \qquad \langle S_r \rangle = v_s. \tag{14}$$

One observes that they couple differently to the Higgs doublet as well as the fermion sector. For instance, the coupling κ_{SH} only couples the CP-even part to the doublet but not the CP-odd part (which would be a CP-violating interaction). Thus, the CP-even and -odd interactions will behave differently under the RGE running and result in different couplings for the CP-even and -odd components in the low-energy Lagrangian. In this basis Eq. (5) becomes

$$V(H, S) \equiv V(H, S_i, S_r)$$

$$= m_H^2 HH^\dagger + \frac{\lambda_H}{2}(HH^\dagger)^2 + \frac{m_{S_r}^2}{2}S_r S_r$$

$$+ \frac{\lambda_{S_r}}{8}(S_r S_r)^2 + \frac{m_{S_i}^2}{2}S_i S_i + \frac{\lambda_{S_i}}{8}(S_i S_i)^2$$

$$+ \frac{\lambda_{S_{ri}}}{4}S_r S_r S_i S_i + \frac{\lambda_{SH_r}}{2}S_r S_r HH^\dagger$$

$$+ \frac{\lambda_{SH_i}}{2}S_i S_i HH^\dagger + \sqrt{2}\kappa_{SH_r}S_r HH^\dagger$$

$$- \frac{3}{\sqrt{2}}\kappa_{S_{ri}}S_r S_i S_i + \frac{1}{\sqrt{2}}\kappa_{S_r}S_r S_r S_r. \tag{15}$$

Using this parametrization we do not only account correctly for RGE effects, but also include operators like

$S|S|^2 +$ H.c.,[3] that are nonexistent in the NMSSM at tree level but generated at the one-loop order. This is because a matching of Eq. (15) already involves the most general CP-conserving potential.

The 2×2 mass matrix of the CP-even eigenstates reads

$$\mathbf{m}_H^2 = \begin{pmatrix} m_{11}^2 & m_{12}^2 \\ m_{12}^2 & m_{22}^2 \end{pmatrix}, \tag{16}$$

with the components

$$m_{11}^2 = \lambda_H v_{\mathrm{SM}}^2,$$

$$m_{12}^2 = \sqrt{2}v_{\mathrm{SM}}\kappa_{SH_r} + v_{\mathrm{SM}}v_s\lambda_{SH_r}, \quad \text{and}$$

$$m_{22}^2 = -\frac{v_{\mathrm{SM}}^2\kappa_{SH_r}}{\sqrt{2}v_s} + \frac{3v_s\kappa_{S_r}}{\sqrt{2}} + v_s^2\lambda_{S_r}, \tag{17}$$

where tree-level tadpole conditions have been used to eliminate m_H^2 and $m_{S_r}^2$. The eigenvalues m_h^2/m_s^2 of $\mathbf{m}_H^2$ are associated with the squared masses of the doublet- and singletlike mass eigenstates. The CP-odd state has the mass

$$m_a^2 = m_{S_i}^2 + \frac{\lambda_{S_i}^2 v_{\mathrm{SM}}^2}{2} - 3\sqrt{2}\kappa_{S_{ri}}v_s + \frac{\lambda_{S_{ri}}v_s^2}{2}. \tag{18}$$

Since we did not assume a CP-violating vacuum, the $m_{S_i}^2$ contribution in Eq. (18) cannot be eliminated (in contrast to $m_{S_r}^2$). However, if we neglect for a moment the RGE running to the matching scale, we can identify $m_{S_i}^2$ with $m_{S_r}^2$ before using the tadpole equations[4] and find

$$m_a^2 \xrightarrow{M_{\mathrm{SUSY}} \to v_{\mathrm{SM}}} -\frac{9v_s^2\kappa_S + v_{\mathrm{SM}}^2\kappa_{SH}}{\sqrt{2}v_s}, \tag{19}$$

which shows that complex singlet extensions with a $\mathbb{Z}_2$ symmetry, i.e., κ_S, $\kappa_{SH} \to 0$, suffer from a massless pseudoscalar Goldstone boson.

In the fermionic sector we find the following mass as well as interaction terms with scalars:

$$\mathcal{L}_{\mathrm{fermion}} = Y_d^{\overline{\mathrm{MS}}}qH^\dagger d - Y_u^{\overline{\mathrm{MS}}}qH - Y_e^{\overline{\mathrm{MS}}}lHe - g_2^u\tilde{H}_uH^\dagger\tilde{W}$$

$$- \frac{g_1^u}{\sqrt{2}}\tilde{H}_uH^\dagger\tilde{B} - g_2^d\tilde{H}_dH\tilde{W} - \frac{g_1^d}{\sqrt{2}}\tilde{H}_dH\tilde{B}$$

$$- Y_S^u\tilde{S}\tilde{H}_uH^\dagger - Y_S^d\tilde{S}\tilde{H}_dH - Y_{\tilde{S}}\tilde{S}\tilde{S}S - \frac{Y_{ud}}{\sqrt{2}}S\tilde{H}_u \cdot \tilde{H}_d$$

$$- \frac{M_{\tilde{g}}}{2}\tilde{g}\tilde{g} - \frac{M_{\tilde{B}}}{2}\tilde{B}\tilde{B} - \frac{M_{\tilde{W}}}{2}\tilde{W}\tilde{W} + \text{H.c.}, \tag{20}$$

---

[3]This operator is actually linearly dependent to κ_{S_r} and $\kappa_{S_{ri}}$. Likewise, all other *primed* couplings in Eq. (5) are linearly dependent.

[4]This will be discussed in more detail later; see Eq. (21).

TABLE I. Parameter counting contributing to the light scalar masses in the (split) NMSSM as well as the SSM.

		Σ
UV	$\lambda,\ \kappa,\ T_\lambda,\ T_\kappa,\ \tan\beta$	5
EFT	$\lambda_H,\ \lambda_S,\ \lambda_{SH},\ \kappa_S,\ \kappa_{SH}$	5

which is analogous to the split MSSM Lagrangian in Ref. [34] extended by a singlet fermion $\tilde{S}$ and scalar S. The splitting of S into its CP-even and -odd parts and the introduction of independent couplings was also performed in the Yukawa sector. However, the different Yukawa couplings are not of particular interest for this paper. To keep the notation simple, we always refer to the Yukawa coupling to the CP-even singlet component, if not stated elsewhere. It is important to stress that all Lagrangian parameters are independent of each other from the viewpoint of the simplified model, even if the notation indicates their relation given above the matching scale. In order to sum up this part, we show in Table I the five free parameters (excluding the VEVs) contributing at tree level to the light scalar masses in the NMSSM as well as in the SSM.

C. One-loop matching

At the matching scale M_{SUSY}, the fields S_r and S_i are contained in the complex singlet S. Thus, they are degenerate in mass and couple identically. Therefore, we have the following additional *matching* relations:

$$
\begin{aligned}
\kappa_{SH} &\equiv \kappa_{SH_r}, \\
\kappa_S &\equiv \kappa_{S_r} = \kappa_{S_{ri}}, \\
\lambda_S &\equiv \lambda_{S_{ri}} = \lambda_{S_i} = \lambda_{S_r}, \\
\lambda_{SH} &\equiv \lambda_{SH_r} = \lambda_{SH_i}, \quad \text{and} \\
m_S^2 &\equiv m_{S_r}^2 = m_{S_i}^2,
\end{aligned}
\tag{21}
$$

which restore the complex-singlet structure at the matching scale. Thus, the information about all heavy SUSY states is encoded in a small set of effective parameters κ_{SH}, κ_S, λ_S, λ_{SH} and λ_H which we need to calculate as precisely as possible. It was already mentioned in the introduction that a tree-level matching is no longer sufficient because of the precise LHC measurements of the Higgs boson mass. For this reason, we use the computer tool SARAH (version 4.14.1) [35–38], which was extended to be able to perform a matching of the scalar sector of two theories at next-to-leading order; see Ref. [22] for more details.

The scalar quartic and trilinear effective couplings are given through NMSSM D and F terms as well as one-loop corrections at the matching scale M_{SUSY}:

$$
\lambda_H = \frac{1}{4}(g_2^2 + g_1^2)\cos^2 2\beta + \frac{1}{2}\lambda^2\sin^2 2\beta + \delta^{(1)}\lambda_H,
$$

$$
\lambda_S = 2\kappa^2 + \delta^{(1)}\lambda_S,
$$

$$
\lambda_{SH} = \lambda^2 - \frac{2\kappa\lambda t_\beta}{1 + t_\beta^2} - \frac{T_\lambda^2}{m_A^2}\left(\frac{t_\beta^2 - 1}{t_\beta^2 + 1}\right)^2 + \delta^{(1)}\lambda_{SH},
$$

$$
\kappa_S = \frac{1}{3}T_\kappa + \delta^{(1)}\kappa_S,
$$

$$
\kappa_{SH} = -T_\lambda\frac{t_\beta}{1 + t_\beta^2} + \delta^{(1)}\kappa_{SH},
\tag{22}
$$

where the shorthand notation $t_\beta = \tan\beta$ is used. The coupling λ_{SH} receives additional nonlocal contributions from tree-level diagrams with one internal heavy Higgs boson shown in the left diagram of Fig. 6. The $\delta^{(1)}$ terms denote the one-loop corrections to the shown tree-level contributions. However, the expressions are rather lengthy while the calculation using SARAH is relatively simple and can be reproduced on any standard personal computer. Thus, we refrain from showing them here.[5]

The one-loop matching of Yukawa couplings is only required for the Higgs boson mass calculation when a running above the NMSSM scale M_{SUSY} is considered. However, we will not consider such a scenario here; i.e., only the tree-level matching conditions are required:

$$
\begin{aligned}
g_1^u &= g_1\sin\beta, & g_2^u &= g_2\sin\beta, \\
g_1^d &= g_1\cos\beta, & g_2^d &= g_2\cos\beta, \\
Y_{ud} &= \lambda, & Y_{\tilde{S}} &= \kappa, \\
Y_S^d &= \lambda\sin\beta, & Y_S^u &= \lambda\cos\beta, \\
Y_{e,d}^{\overline{\text{MS}}} &= \cos\beta Y_{e,d}^{\overline{\text{DR}}}, & Y_u^{\overline{\text{MS}}} &= \sin\beta Y_u^{\overline{\text{DR}}}, \\
M_{\tilde{B},\tilde{W},\tilde{g}} &= M_{1,2,3}.
\end{aligned}
\tag{23}
$$

We give a brief example for the mass spectrum and the NLO effects in Fig. 2 where we plot the scalar mass spectrum calculated in the EFT at the scale v_{SM} as a function of M_{SUSY}. In a first step of the calculation a running of the effective couplings to the scale M_{SUSY} is carried out, before the matching is performed using Eqs. (22) and (23). Finally, the RGEs run back to v_{SM} and the effective Higgs boson masses are computed at the low scale at two-loop order.[6] All numerical calculations are performed with a SARAH -generated SPHENO [39,40] version which includes the full two-loop RGEs. One can clearly see the significant impact of the NLO corrections: at LO the desired Higgs mass of about 125 GeV is obtained for

---

[5]The expressions can easily be obtained with SARAH using the file Models/SMSSM/Matching_SplitSUSY.m included in the public package.

[6]See Fig. 5 of Ref. [22] for a detailed discussion on the effective Higgs mass calculation.
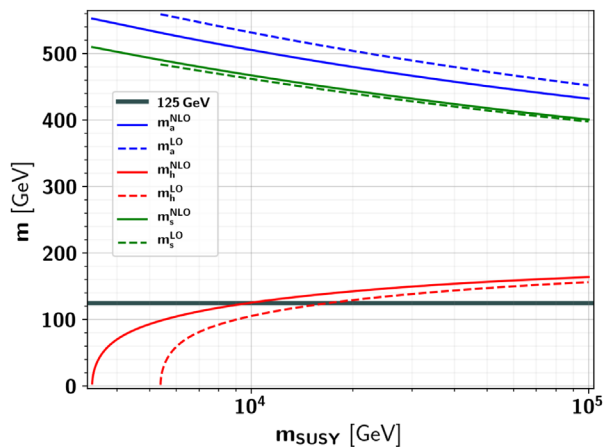
FIG. 2. Example for the scalar spectrum of the split NMSSM. The red straight (dashed) line shows the doubletlike Higgs boson mass as a function of the matching scale using NLO (LO) matching conditions. The mass associated with the CP-even (-odd) state is shown in green (blue). The horizontal line corresponds to the central value of the measured Higgs boson mass. The used parameter values are $M_1 : M_2 : M_3 = 0.15 : 1 : 3$ TeV, $\tan\beta = 5$, $\lambda = \kappa/2 = 0.9$, $T_\lambda = -T_\kappa = 500$ GeV, $A_0 = v_S = 100$ GeV and $m_A = 0.1 M_{\mathrm{SUSY}}$.

M_{SUSY} larger than 10 TeV, while NLO corrections can pull M_{SUSY} below 10 TeV. The impact of higher-order corrections from the matching conditions on the mass spectrum is discussed in further detail in the next section.

III. MATCHING OF MASS PARAMETERS

The previous section showed that higher-order corrections to matching conditions can have a significant impact on the soft-SUSY-breaking scale required for being consistent with the Higgs boson mass measurement. In this section we further examine the behavior of these corrections.

Quartic scalar couplings are dimensionless in $D = 4$ dimensions. Thus, the dependence on the mass scale involved in the matching, M_{SUSY}, is guaranteed to disappear in the limit $M_{\mathrm{SUSY}} \to \infty$. However, this is not the case for parameters with mass dimension greater than zero, which appear in the Lagrangian of the SSM; cf. Eq. (15) and the discussion of Eqs. (6) and (7). A related behavior can be seen explicitly by looking at the one-loop correction to the trilinear self-coupling κ_S at the matching scale, depicted in Fig. 3. The contribution from a heavy Higgs boson in the loop does not decouple, although being independent of the Higgs mass itself, but becomes

$$\delta^{(1)}\kappa_S \simeq -\frac{\kappa\lambda T_\lambda \cos^2 2\beta}{8\pi^2}, \qquad (24)$$

which can easily reach several GeV if $T_\lambda \approx 1$ TeV. As long as the loop corrections are smaller than the tree-level
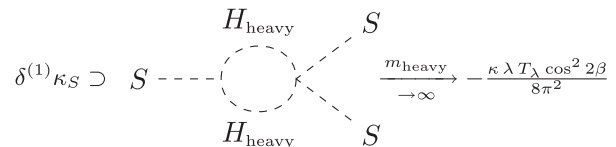

FIG. 3. One-loop contribution to the matching condition of the trilinear singlet self-coupling which does not vanish if $M_{\mathrm{SUSY}} \to \infty$. In this example all masses of the heavy doublet H_{heavy} are assumed to be degenerate at the matching scale M_{SUSY}. All other contributions (i.e., wave function renormalization and triangle diagrams) decouple in this limit.

contributions, one might not worry about this behavior. However, there are various situations which can lead to surprisingly large, but not necessarily unphysical, higher-order corrections to the scalar masses and trilinear couplings. One interesting case is $T_\kappa \simeq 0$, which could either be due to some additional symmetry or just a numerical coincidence. In both cases one would find $\kappa_S \simeq 0$ at tree level at the matching scale. However, if it is just a coincidence or if the symmetry is broken by loop corrections, one would find $|\delta^{(1)}\kappa_S| \gg 0$ if $T_\lambda \neq 0$. Similarly, an accidental symmetry or numerical coincidence could cause a cancellation within the pseudoscalar mass given in Eqs. (18) and (19); i.e., a would be nearly massless at tree level but could receive a sizable mass from different higher-order corrections to κ_S and κ_{SH}. Another factor in this discussion is the RGE running that spoils the identities in Eq. (21) after the matching has been applied. This effect can also lead to an accidental enhancement of higher-order matching conditions if, for instance, a one-loop matching changes the sign of a coupling with respect to the tree-level matching.

In principle, one could avoid the entire discussion about large higher-order corrections by using a renormalization scheme different from the minimal subtraction ($\overline{\mathrm{MS}}$) scheme. In the case of an on-shell (OS) scheme, the masses are fixed to all orders by adding fine-tuned counterterms [41]. However, one might expect that large loop corrections then show up at another place. For instance, large OS counterterms will influence the two-loop corrections in the doublet sector which itself has only very restricted freedom concerning the mass counterterms. Even more important, one would not be allowed to feed these parameters into the RGEs, which are defined for $\overline{\mathrm{MS}}$ parameters only. Therefore, the proper matching is—by now—the most suitable solution to relate the SSM and NMSSM in the most predictive way.

In what follows, we continue with a quantitative discussion of the higher-order corrections. In this context, we do not assume any additional symmetries which would predict tiny or zero T_κ or m_a, respectively. However, we would like to check how likely parameter configurations at the matching scale appear where the NLO correction supersedes the LO contributions. In order

TABLE II. Scan ranges for a random scan over the NMSSM parameter space. All parameters are input at the matching scale $M_{\rm SUSY}$.

Parameter	Scan range
λ	$[-3, 3]$
κ	$[-3, 3]$
$\tan\beta$	$[1, 50]$
$M_{\rm SUSY}$	$[10^3, 10^{16}]$ GeV
m_A	$r \cdot M_{\rm SUSY}$
r	$[0.01, 100]$
T_λ	$[-5000, 5000]$ GeV
T_κ	$[-5000, 5000]$ GeV
$M_{1,2}$	$[10, 3000]$ GeV
M_3	$[1000, 3000]$ GeV
v_S	$[0, 3000]$ GeV
A_0	$[-500, 500]$ GeV

FIG. 4. Relative size of the one-loop corrections to the mass m_s (m_a) of the (pseudo)scalar (a) s in percent and the trilinear singlet-self-coupling κ_{S_r} evaluated at the scale $v_{\rm SM}$ as a function of the ratio of the soft-SUSY-breaking coupling T_λ and the tree-level mass $m_s^{(0)}$ ($m_a^{(0)}$). It is $0 \lesssim |T_\lambda|, m_a^{(0)} \lesssim 5$ TeV and $0.12 \lesssim m_s^{(0)} \lesssim 7$ TeV.

to cover large parts of the parameter space, we perform a random scan according to the ranges in Table II using the generated SPHENO code and require $m_h = (125 \pm 2)$ GeV for the results obtained with NLO matching conditions. Furthermore, we require $M_{\rm SUSY}$ and m_A to be at least twice as large as the largest mass parameter of the low-energy Lagrangian.

In Fig. 4 we show the relative size of the higher-order corrections to the scalar singlet masses m_a and m_s evaluated at the scale $v_{\rm SM}$ when using tree-level [denoted with a (0) label] or one-loop [denoted with a (1) label] matching conditions at the matching scale. The x axis was chosen to show the $T_\lambda/m_{a,s}^{(0)}$ dependence, because T_λ presumably becomes important for the one-loop shift $\delta^{(1)}\kappa_{S_r}$ which itself can have a large impact on the one-loop correction to the tree-level masses of a and s. The color of the points indicates the relative size of the running value of κ_{S_r} at $v_{\rm SM}$ between a tree-level and one-loop matching at $M_{\rm SUSY}$. For m_a a clear correlation with $T_\lambda/m_a^{(0)}$ and $\kappa_{S_r}^{(1)}/\kappa_{S_r}^{(0)}$ is visible. Even for large values of T_λ a relatively small m_a can be realized at tree level by choosing T_κ accordingly; cf. Eqs. (19) and (22). However, at the one-loop order the contributions of Fig. 3 scale with T_λ and can push the loop-corrected masses to up to 10 times larger masses.

A similar behavior is observed for m_s in the lower plot of Fig. 4. However, the dependence on $\kappa_{S_r}^{(1)}/\kappa_{S_r}^{(0)}$ is rather weak and inverted due to the additional contributions from quartic couplings which enhances the dimensionality of the parameter space for m_s and the contribution of κ_{S_r} to $m_s^{(0)}$ enters with a different sign; cf. m_{22} in Eqs. (17) and (18). In addition, the chosen parameter ranges in Table II are not optimized for cases where
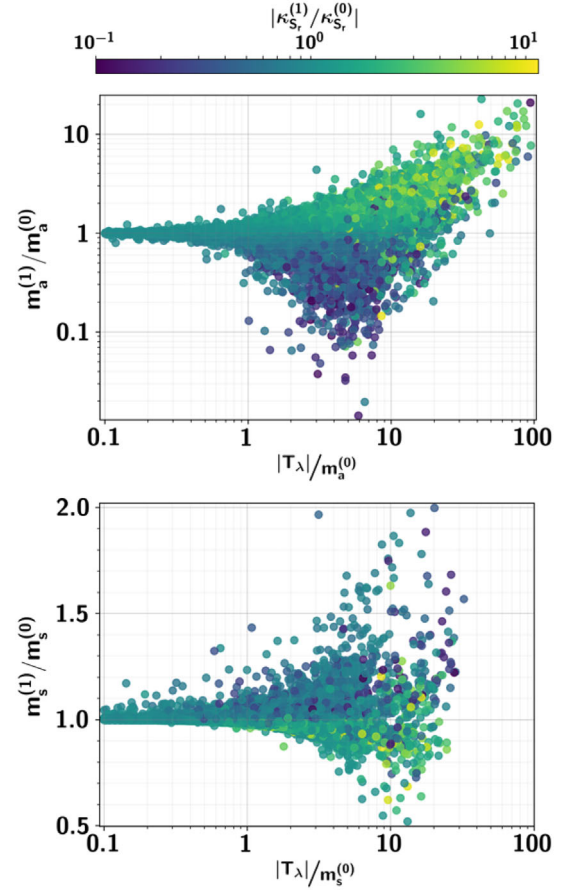
$m_s < m_h$ which have a relatively small parameter space. Thus, we find only rarely points with very light singlets (at tree as well as one-loop level) such that the maximal loop corrections are smaller than for m_a.

It was already discussed that higher-order corrections, that are bigger than the leading-order ones, are not necessarily a sign for the breakdown of perturbation theory but could be caused by accidental cancellations at tree level. In order to check if this is always the case, or if there are strongly coupled parameter points, the most reliable approach is to study the behavior of the two-loop corrections. This is well beyond the scope of this paper, though [41]. Instead, we use a simpler approach and check the tree-level unitarity constraints using SPHENO [42] which are closely connected to perturbativity as discussed in Refs. [43,44]. However, only very few points did not pass the tree-level unitarity constraints. Thus, perturbativity is presumably not in danger but would require further investigations.
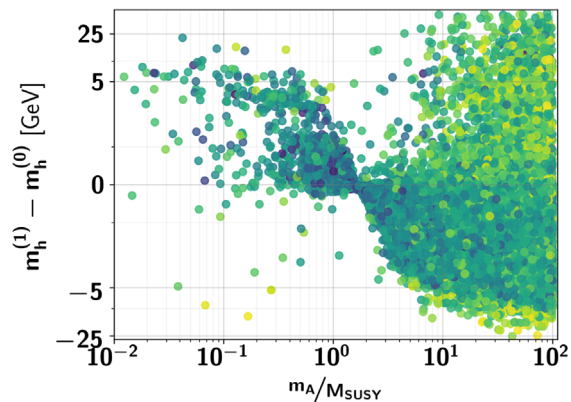
FIG. 5.   Absolute difference in the prediction of the Higgs boson mass using LO and NLO matching conditions as a function of the ratio of the two mass scales that are characteristic for sfermions and heavy Higgs bosons. All shown points fulfill the Higgs boson mass constraint within a 2 GeV interval.

We close the discussion of higher-order corrections with the SM-like Higgs boson mass corrections shown in Fig. 5. In this plot we depict the absolute Higgs boson mass correction as a function of the ratio of the heavy-Higgs mass scale m_A and the matching scale M_{SUSY} and the absolute difference in the coupling κ_{SH_r} at v_{SM} when using a tree-level or a one-loop matching. The ratio m_A/M_{SUSY} appears logarithmically in the matching conditions and becomes crucial for the uncertainty of the higher-order corrections for large values. We observe a negative (positive) shift on the Higgs boson mass for larger (smaller) ratios. Varying the two scales around 4 orders of magnitude leads to changes in the Higgs boson mass corrections of more than ± 25 GeV. Thus, a tower of EFTs using e.g., an intermediate matching to a singlet extended 2HDM would be more reliable if $m_A/M_{\mathrm{SUSY}} \ll 1$. In addition to a logarithmic enhancement, diagrams containing a heavy-Higgs propagator with a down-type sfermion loop attached can yield an enhancement by positive powers of $\tan\beta$; see for instance the right diagram in Fig. 6. Although κ_{SH_r} receives similar contributions like κ_{S_r} in Eq. (24), the dependence of m_h on κ_{SH_r} is not as strong as the dependence of $m_{a,s}$ to κ_{S_r}. This is due to the fact that
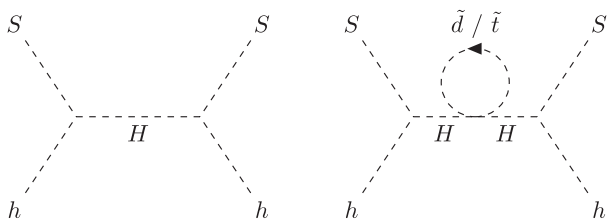

FIG. 6.   Left diagram: Example of a nonlocal contribution to the tree-level matching of λ_{SH}. Right: Example of a $\tan\beta$-enhanced (-suppressed) one-loop diagram involving a sbottom (top squark) loop and two heavy Higgs boson propagators.

κ_{SH_r} already depends on T_λ at tree level such that the relative size of $\kappa_{SH_r}^{(0)}$ and $\kappa_{SH_r}^{(1)}$ is rather small. Nevertheless, the impact on the Higgs boson mass

$$m_h^2 \propto v_S \kappa_{SH_r}^{(1)} \qquad (25)$$

can be sizable for large values of T_λ and v_S.

Despite the logarithmic enhancement, we assume that a one-scale matching is still precise enough for the considered spread between the two scales. To answer this question more precisely, a comparison with the two possible EFT towers is required which is beyond the scope of this paper.

IV. MATCHING VS SIMPLIFIED MODELS

Table I counts the same number of free parameters contributing to the light scalar masses in the NMSSM as well as the SSM. Thus, one may ask about the advantage of the matching since the dimensionality of the parameter space is not reduced. However, it will be shown that SUSY relations are still active, even if the matching scale is much higher than the electroweak scale. This leads to significant constraints on certain parameter regions in the EFT.

A parameter scan according to Table II was performed using the high-scale version of SPHENO as described in Sec. III. In addition to the checks performed with SPHENO, i.e., ρ-parameter and tree-level unitarity, we use MICROMEGAS (version 5.0.2) [45] to calculate the relic density. Since MICROMEGAS is based on the tree-level tool CALCHEP [46], the theoretical uncertainty of Ωh^2 is quite high [47]. Thus, we require $\Omega h^2 = 0.12 \pm 0.08$. Furthermore, we use HIGGSBOUNDS (version 4.3.1) [48–50], which compares the computed masses, cross sections and branching fractions against publicly available Higgs searches. In addition to the Higgs boson mass constraints we also require the lightest chargino to be heavier than 94 GeV and a gluino heavier than 1.5 TeV.

SPHENO also offers the possibility to be executed with low-scale input only, i.e., to perform all low-energy calculations at fixed order using direct inputs for all Lagrangian parameters in Eqs. (5) and (20). For the comparison, a second random scan is performed using this low-scale mode of SPHENO which is equivalent to common simplified-model approaches. In order to produce a comparable parameter set for the SSM, the scan ranges for the low-energy parameters are chosen from the minimum and maximum values that were the outcome of the high-scale scan. It should be noted that this procedure is already much more restrictive than usual parameter scans of simplified models, where typically all coupling values allowed by perturbative unitarity are included. The unitarity constraints in the limit of a large scattering energy s and negligible differences between the couplings of the CP-even and -odd singlet are
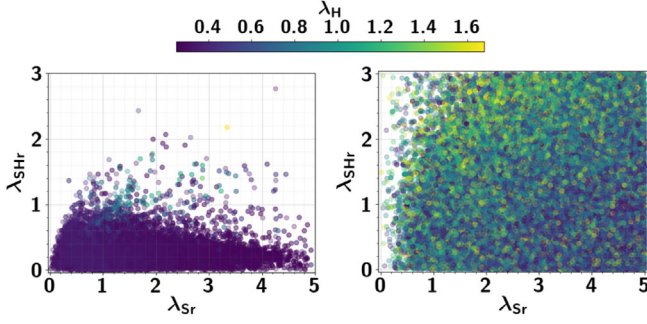
FIG. 7. Quartic couplings of the matched EFT (left) and the simplified model (right) both evaluated at the scale v_{SM}.

$$8\pi > \max\left\{|\lambda_H|, |\lambda_S|, |\lambda_{SH}|,\right.$$

$$\left.\frac{1}{2}\left|3\lambda_H + 2\lambda_S \pm \sqrt{9\lambda_H^2 + 8\lambda_{SH}^2 - 12\lambda_H\lambda_S + 4\lambda_S^2}\right|\right\}. \quad (26)$$

If only one of these coupling is large, this corresponds to

$$|\lambda_H^{\mathrm{uni}}| < \frac{8}{3}\pi \simeq 8.4, \qquad |\lambda_S^{\mathrm{uni}}| < 4\pi \simeq 12.6,$$

and $\quad |\lambda_{SH}^{\mathrm{uni}}| < 4\sqrt{2}\pi \simeq 17.8, \quad (27)$

which needs to be compared with the range

$$|\lambda_H^{\mathrm{EFT}}| \lesssim 1.6, \qquad |\lambda_S^{\mathrm{EFT}}| \lesssim 5, \qquad |\lambda_{SH}^{\mathrm{EFT}}| \lesssim 3, \quad (28)$$

predicted by the matching. Thus, a conventional simplified-model approach would have to investigate a parameter space with a volume which is roughly 80 times larger than those of an NMSSM-inspired EFT scan (concerning the subspace of these three couplings only). Moreover, in the following we show that this ratio is actually even larger.

In Fig. 7 we show the correlation between the three quartic couplings λ_H, λ_{S_r}, and λ_{SH_r} evaluated at the scale v_{SM}. If a proper matching is performed (left plot), we observe that λ_H is small since it is mainly given by D-term contributions. F terms could in principle lead to an enhancement in λ_H but would also enhance $\lambda_{SH_r} \propto \lambda(\lambda - \kappa)$. Thus, the singlet-doublet admixture would increase which is already constrained by LHC measurements; i.e., such points do not pass the HIGGSBOUNDS checks. The singlet self-coupling λ_{S_r} is hardly constrained because it affects only the BSM part of the scalar sector as well as the singlino mass for which no constraint exists.

In comparison, the right plot in Fig. 7 gives the results for the low-scale scan. We observe only very weak correlations among the three quartic couplings. In this case, the collider constraints are the only limiting factor, since the scalar couplings are assumed to be independent of each other as well as of the fermion sector. Thus, a very large fraction of the parameter space forbidden by SUSY is opened.
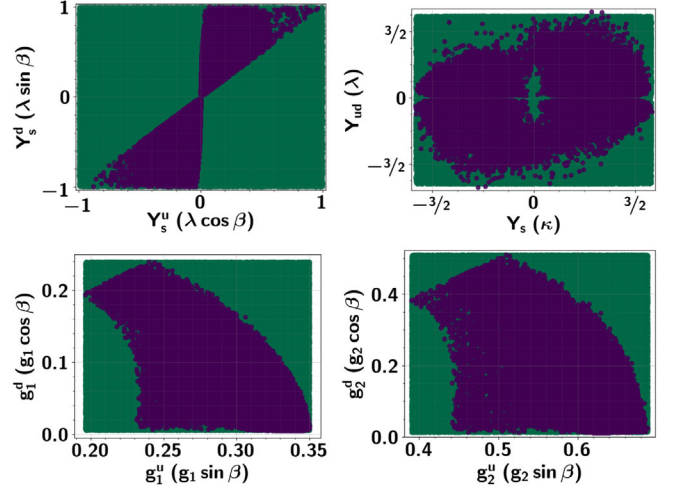

FIG. 8. Yukawa couplings of the matched EFT (purple) and the simplified model (green) both evaluated at the scale v_{SM}. The expressions in parentheses are the corresponding tree-level matching conditions as they are applied at the matching scale.

For very large values of λ_{SH_r} we observe a correlation to λ_H which implies large cancellations in the Higgs boson mass in order to achieve a 125 GeV Higgs boson.

The comparison between the two approaches can also be extended to the fermion sector. In Fig. 8 we compare all relevant Yukawa couplings determined with and without the matching to the NMSSM. Also in this case the EFT approach is actually only compared with a small fraction of the parameter space of the simplified model because we are much more restrictive than perturbative unitarity. We observe that the chargino constraint is not enough to overcome the large freedom in this sector such that the Yukawa couplings in the simplified model are completely unconstrained. However, during the matching, SUSY properties not only give relations among different fermionic couplings, but also transmit many experimental and theoretical constraints from the Higgs to the Yukawa sector. Consequently, a significant fraction of the parameter space is not accessible anymore.

From the considerations on the Lagrangian parameters one can go one step further and ask the question whether it would be possible to experimentally distinguish between a SUSY-inspired and a pure singlet extension. This question was already answered positively in Ref. [28] based on an analysis of the signal strength of Higgs-to-Higgs decays in the CxSM[7] compared to the NMSSM. However, the analysis of the SSM collider phenomenology is beyond the scope of this paper. Furthermore, Ref. [29] compared DM production in the MSSM with a simplified model. Also in this comparison, the latter could not reproduce all

---

[7]This is a complex-singlet extension of the SM with an additional $\mathbb{Z}_2$ symmetry.
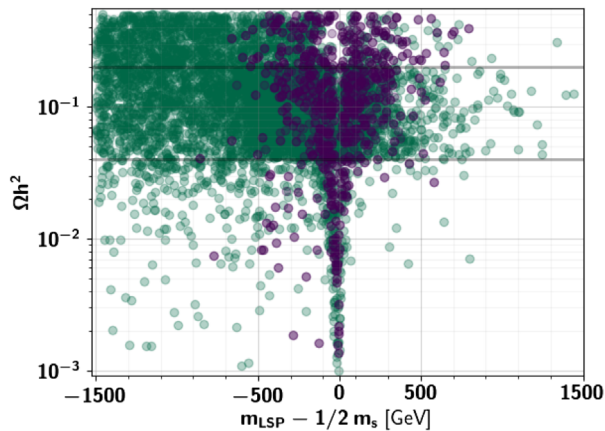
FIG. 9.   Prediction of the relic density using MICROMEGAS as a function of the difference between the singletlike LSP mass and the *CP*-even scalar singlet in the simplified model (green) and the matched EFT (purple). The horizontal lines enclose the region $0.04 < \Omega h^2 < 0.2$ onto which we cut in Figs. 7 and 8. In this plot we require at least 90% singlet admixture in the LSP.

phenomenological properties of the supersymmetric UV completion.

In contrast to simplified models, SUSY models give hints whether additional states are likely to be found because their mass is close to the one of the scalar singlet. For instance, when requiring the lightest supersymmetric particle (LSP) to be a pure singlino, its mass will correlate with the singlet *CP*-even mass. This scenario is attractive because it provides an additional mechanism to avoid a relic density overabundance through resonant annihilation of two DM singlinos into a singletlike scalar boson compared to the annihilation mechanism in the MSSM. In Fig. 9 we compare this mechanism in both approaches with and without matching. We plot the relic density as a function of the mass splitting $\Delta = m_{\rm LSP} - 1/2 m_s$ while requiring a singlino fraction for the LSP of at least 90%. Consequently Ωh^2 steeply drops near $\Delta = 0$ in both approaches. However, one can also see that Δ can be $\mathcal{O}(\rm TeV)$ in the simplified model and still be consistent with the dark matter observation. In contrast, the matching predicts the two particles to appear within a range of at most 500 GeV in order to get a viable dark matter scenario.

Furthermore, if the LSP is Higgsino-like, one can achieve a resonant annihilation via an s-channel exchange of a *CP*-odd scalar (with appropriate mixing). However, this channel is only mildly constrained by the matching conditions because the *CP*-odd singlet mass is determined by the trilinear soft-breaking couplings while the Higgsino masses scale with $\propto v_s \lambda$.

V. CONCLUSION AND OUTLOOK

Simplified models are a widely used method to study specific features of BSM physics. It is often assumed that these models can arise as the low-energy limit of one or even several fundamental UV theories. However, we pointed out that the choice of a concrete UV model can lead to tremendous constraints on the parameter space of simplified models. We have shown for the specific example of the singlet extended SM embedded in a SUSY framework that the full theory always predicts additional light particles to be present. Thus, simplified models do not have the same power in giving advise for further experimental searches as the full theory has. Moreover, even if all light states are included in the EFT, the predictions between a simplified study assuming only the parameters at the weak scale and a full analysis including the proper matching to the UV theory can be very different. We have shown for several examples that the relations between the parameters originating in the UV theory still give large constraints on the accessible parameter space. This is even the case when there is a large separation between the weak scale and the scale where the other d.o.f. of the full theory are located. Thus, one needs to make a case by case decision if the usage of simplified models for a specific study is justified, or if the matching to the full theory should be included.

If the matching between the EFT and UV theory is considered, the calculation must be done with the necessary precision. We discussed the impact of higher-order corrections of matching conditions onto the scalar mass spectrum in our chosen setup. We have shown that the effects in the singlet sector can be very large under specific conditions. This is in particular the case when there is an accidental cancellation at tree level. In these cases the prediction for the pseudoscalar mass can change by one order of magnitude. As we have discussed, this is *not* a sign of the breakdown of perturbation theory.

This work might deal as guideline for future studies: we have concentrated here on one specific example for the UV and EFT. However, also other low-energy limits of the (split)-NMSSM are possible, e.g., real singlet extended SM, the 2HDM complemented with a real or complex singlet, or just a 2HDM. In addition, contributions from higher-dimensional operators were neglected, based on experiences from high-scale MSSM. To verify these results for the split NMSSM, the impact of operators like e.g., $S^4 HH^\dagger$ and $S^3 HH^\dagger$ onto the SM-like Higgs boson mass needs to be investigated.

[1] S. Chatrchyan *et al.* (CMS Collaboration), Phys. Lett. B **716**, 30 (2012).

[2] G. Aad *et al.* (ATLAS Collaboration), Phys. Lett. B **716**, 1 (2012).

[3] G. Aad *et al.* (ATLAS and CMS Collaboration), Phys. Rev. Lett. **114**, 191803 (2015).

[4] A. M. Sirunyan *et al.* (CMS Collaboration), J. High Energy Phys. 05 (2018) 025.

[5] J. D. Wells, in *Proceedings of the 11th International Conference on Supersymmetry and the Unification of Fundamental Interactions (SUSY 2003), Tucson, Arizona* (2003), https://inspirehep.net/search?p=find+eprint+hep-ph/0306127.

[6] N. Arkani-Hamed, S. Dimopoulos, G. F. Giudice, and A. Romanino, Nucl. Phys. **B709**, 3 (2005).

[7] N. Arkani-Hamed and S. Dimopoulos, J. High Energy Phys. 06 (2005) 073.

[8] G. F. Giudice and A. Romanino, Nucl. Phys. **B699**, 65 (2004); **B706**, 487(E) (2005).

[9] S. V. Demidov and D. S. Gorbunov, J. High Energy Phys. 02 (2007) 055.

[10] S. V. Demidov, D. S. Gorbunov, and D. V. Kirpichnikov, J. High Energy Phys. 11 (2016) 148; 08 (2017) 080.

[11] S. V. Demidov, D. S. Gorbunov, and D. V. Kirpichnikov, Phys. Lett. B **779**, 191 (2018).

[12] J. Pardo Vega and G. Villadoro, J. High Energy Phys. 07 (2015) 159.

[13] P. Athron, J.-h. Park, T. Steudtner, D. Stöckinger, and A. Voigt, J. High Energy Phys. 01 (2017) 079.

[14] E. Bagnaschi, J. Pardo Vega, and P. Slavich, Eur. Phys. J. C **77**, 334 (2017).

[15] F. Staub and W. Porod, Eur. Phys. J. C **77**, 338 (2017).

[16] B. C. Allanach and A. Voigt, Eur. Phys. J. C **78**, 573 (2018).

[17] H. E. Haber and R. Hempfling, Phys. Rev. D **48**, 4280 (1993).

[18] M. Beneke, P. Ruiz-Femenia, and M. Spinrath, J. High Energy Phys. 01 (2009) 031.

[19] M. Gorbahn, S. Jager, U. Nierste, and S. Trine, Phys. Rev. D **84**, 034030 (2011).

[20] G. Lee and C. E. M. Wagner, Phys. Rev. D **92**, 075032 (2015).

[21] H. Bahl and W. Hollik, J. High Energy Phys. 07 (2018) 182.

[22] M. Gabelmann, M. Muehlleitner, and F. Staub, Eur. Phys. J. C **79**, 163 (2019).

[23] H. Bahl, in *Proceedings of 54th Rencontres de Moriond on QCD and High Energy Interactions (Moriond QCD 2019), La Thuile, Italy* (2019), https://inspirehep.net/search?p=find+eprint+1905.04918.

[24] D. Alves (LHC New Physics Working Group), J. Phys. G **39**, 105005 (2012).

[25] R. Contino, M. Ghezzi, C. Grojean, M. Muhlleitner, and M. Spira, J. High Energy Phys. 07 (2013) 035.

[26] R. Costa, A. P. Morais, M. O. P. Sampaio, and R. Santos, Phys. Rev. D **92**, 025024 (2015).

[27] D. Buttazzo, F. Sala, and A. Tesi, J. High Energy Phys. 11 (2015) 158.

[28] R. Costa, M. Mühlleitner, M. O. P. Sampaio, and R. Santos, J. High Energy Phys. 06 (2016) 034.

[29] C. Borschensky, G. Coniglio, and B. Jäger, Eur. Phys. J. C **79**, 428 (2019).

[30] S. P. Martin, Adv. Ser. Dir. High Energy Phys. **18**, 1 (1998).

[31] M. Maniatis, Int. J. Mod. Phys. A **25**, 3505 (2010).

[32] U. Ellwanger, C. Hugonie, and A. M. Teixeira, Phys. Rep. **496**, 1 (2010).

[33] M. D. Goodsell, K. Nickel, and F. Staub, Phys. Rev. D **91**, 035021 (2015).

[34] E. Bagnaschi, G. F. Giudice, P. Slavich, and A. Strumia, J. High Energy Phys. 09 (2014) 092.

[35] F. Staub, Comput. Phys. Commun. **181**, 1077 (2010).

[36] F. Staub, Comput. Phys. Commun. **182**, 808 (2011).

[37] F. Staub, Comput. Phys. Commun. **184**, 1792 (2013).

[38] F. Staub, Comput. Phys. Commun. **185**, 1773 (2014).

[39] W. Porod, Comput. Phys. Commun. **153**, 275 (2003).

[40] W. Porod and F. Staub, Comput. Phys. Commun. **183**, 2458 (2012).

[41] J. Braathen and S. Kanemura, Phys. Lett. B **796**, 38 (2019).

[42] M. D. Goodsell and F. Staub, Eur. Phys. J. C **78**, 649 (2018).

[43] M. E. Krauss and F. Staub, Eur. Phys. J. C **78**, 185 (2018).

[44] F. Staub, Phys. Lett. B **789**, 203 (2019).

[45] G. Bélanger, F. Boudjema, A. Goudelis, A. Pukhov, and B. Zaldivar, Comput. Phys. Commun. **231**, 173 (2018).

[46] A. Pukhov, arXiv:hep-ph/0412191.

[47] P. Bergeron, P. Sandick, and K. Sinha, J. High Energy Phys. 05 (2018) 113.

[48] P. Bechtle, O. Brein, S. Heinemeyer, G. Weiglein, and K. E. Williams, Comput. Phys. Commun. **181**, 138 (2010).

[49] P. Bechtle, O. Brein, S. Heinemeyer, G. Weiglein, and K. E. Williams, Comput. Phys. Commun. **182**, 2605 (2011).

[50] P. Bechtle, O. Brein, S. Heinemeyer, O. Stal, T. Stefaniak, G. Weiglein, and K. E. Williams, Eur. Phys. J. C **74**, 2693 (2014).